ELSEVIER

Contents lists available at ScienceDirect

# Materials Science and Engineering A

journal homepage: www.elsevier.com/locate/msea



## Effect of alloying on the structural properties of Sn-based alloys

F. Abd El-Salam, R.H. Nada, A.M. Abd El-Khalek\*, M.R. Nagy, R. Abd El-Hasaab

Physics Department, Faculty of Education, Ain Shams University, Cairo, Egypt

#### ARTICLE INFO

Article history: Received 17 October 2009 Received in revised form 10 January 2010 Accepted 11 January 2010

PACS: 61.66.Dk 62.20.–x 62.40.+i

Keywords:
Rapid solidification
Normal cast
Microstructure
Intermetallic compound
Ternary alloy
Precipitates

#### ABSTRACT

Sn alloyed separately with Zn, Sb, Bi (all of purity 99.99% and the same percent 8.6 wt.%) was prepared either by normal cast or rapid solidification from the melt. X-ray diffraction patterns, DTA thermographs and Doppler broadening profiles were obtained for all the samples under the same conditions. The measurements of lattice strain, crystallite size, melting point, specific heat, the density of valence (free) electrons and the probability of trapping the free positrons showed deviations from the surface activity theory depending on the alloying element and the method of preparation. The formation of intermetallic compounds highly affects the strength of the alloys.

© 2010 Elsevier B.V. All rights reserved.

### 1. Introduction

Real crystals are far from being perfect because they contain either the lattice defects or impurity defects [1], which control their properties. The nature of the formed microstructure due to the method of preparation controls to a high degree, the mechanical properties of the tested samples.

Rapid solidification improves the mechanical properties [2] and the structure obtained shows less variability [3], new intermediate phases [4], fine microstructure [5] and extended solubility [6].

X-ray diffraction analysis enables the determination of crystallite size, lattice strain and identifying the existing intermediate compounds. DTA, which is a dynamic method in which equilibrium conditions are not attained [7], used to study phase transformation.

The information contained in Doppler broadening studies [8] are its effect on the line shape of annihilation radiation which differs for different materials and is also sensitive to positron trapping by lattice defects.

The present work aims to clarify the microstructure variations caused by the different alloying elements and the preparation method through the analysis of the obtained diffractograms, ther-

\* Corresponding author. E-mail address: Asaad\_abdelkahlk@yahoo.com (A.M. Abd El-Khalek). mograms and the effect of Doppler broadening variations on the line shape of annihilation radiation.

#### 2. Experimental

The tested Sn-based alloys were prepared from the alloying materials Zn, Sb, and Bi each of purity 99.99% and 8.6 wt.%. The investigated alloys were prepared by weighting for each alloy the proper ratios of their components together with a CaCl<sub>2</sub> flux, to avoid oxidation, and each alloy was melt in graphite crucible placed in the stable zone of an electric furnace adjusted at a temperature at least 50 K above the melting point. The casting was carried out in iron moulds. The melt was finally cooled to room temperature then remelt under the same conditions. The melting period was about 1 h and the melting process was repeated three times. The ingot was given a homogenizing vacuum anneal at 423 K for 47 h and slowly cooled to room temperature. The ingots were swaged and cold drawn into wires of 0.8 mm in diameter and disc-shaped (sheets) samples 1.5 mm thick 8 mm width and 87 cm long. The samples were annealed in a tubular furnace provided with a thermoregulator keeping the temperature constant for several hours within  $\pm 2$  K.

Rapid solidification from the melt was achieved by using a single type melt-spinning technique. The metallic ribbons were obtained by a process in which a molten alloy jet impinges with a substrate surface rotating at about 5000 rpm which continuously chills the

melt and transport the chilled materials away from the melt. The ribbons were treated such that each ribbon has 0.3–0.5 cm width, 0.1–0.18 mm thick and 5–7 cm long by using knife cutter.

The interplanar spacing d of a plane (hkl) can be determined from Bragg's law [9]:

$$n\lambda = 2d\sin\theta\tag{1}$$

where n is the order of diffraction = 1, 2...n, and is commonly taken as unity,  $\lambda$  is the wavelength of the used X-ray source, and  $\theta$  is the Bragg angle.

A Shimadzu X-ray diffractometer (Dx-30) was used to trace the structural variations in the samples by analyzing the obtained patterns. The X-ray tube giving copper ( $K_{\alpha}$ ) radiation operated at 30 kV and 30 mA emits X-ray beam of wavelength  $\lambda$  = 0.15406 nm, the divergence slit is 1°, the scatter slit is 1° and the receiving slit is 0.1 mm. The scanning followed county mode with  $\theta$  = 2 $\theta$  as drive axis, scan range 6.000–90.000, scan speed 8°/min, sampling pitch 0.16°, preset time 0.4 s full-scale 0.5 kcps. The smoothing points are 5 and the background was automatically subtracted.

DTA measurements above room temperature were performed using Shimadzu DTA-30B series. The specimen weight was about 20-25 mg, the heating rate was set at  $10\,\mathrm{K/min}$  starting from  $298\,\mathrm{K}$  (the room temperature) up to  $773\,\mathrm{K}$ .

The Doppler broadening was measured by using hyperpure Ge gamma detectors. In the so-called source-sample-sandwich arrangement used the positron source is placed between two identical samples. The typical resolution of the Ge detector used is around 1.1 keV at 511 keV. This is considerably compared to the width of 23 keV of the annihilation peak which means that the experimental line shape is strongly influenced by the detector resolution. The energy distribution is characterized by the "line shape parameter" S which is defined as the sum of counts in a central part of the peak relative to the total peak counts.

#### 3. Results

Equilibrium phase diagrams for the tested Sn–Zn, Sn–Sb and Sn–Bi alloys are given in Fig. 1(a–c). X-ray diffraction patterns obtained for the matrix Sn and these alloys prepared either by normal cast (N) or by rapid cooling, (R) samples, are given in Fig. 2(a–g).

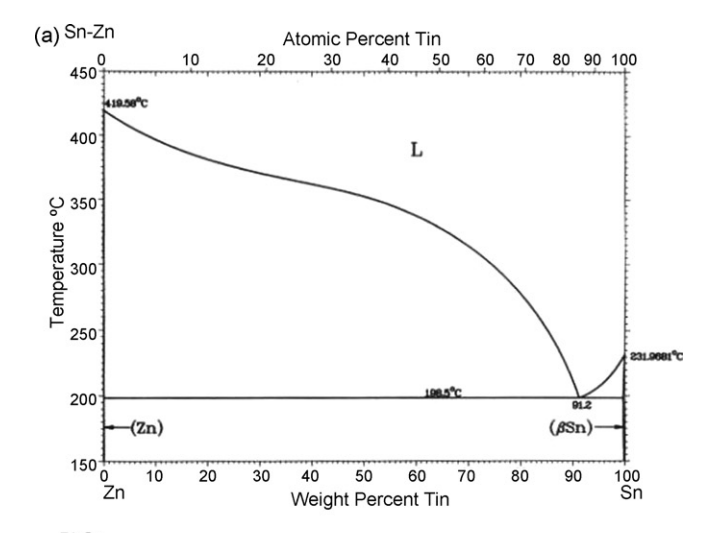
The calibrations of the X-ray diffractometer was carried out by obtaining the full width at half maximum intensity for the sample,  $\beta_s$ , and the quartz (taken as reference),  $\beta_r$ , and using the relation  $\beta_{\text{corr.}} = \sqrt{\beta_r - \beta_s}$  to obtain the corrected,  $\beta_{\text{corr.}}$ , to get the corrected crystallite size,  $\eta$ , from the relation  $\eta = (0.95\lambda/\beta_{\text{corr.}}\cos\theta)$ . The diffraction rays breadth B is therefore affected by the breadth  $B_\eta$  due to the crystallite size, which is obtained from the full width at half maximum (FWHM) intensity in radians and  $B_\varepsilon$  due to lattice strain size [10].

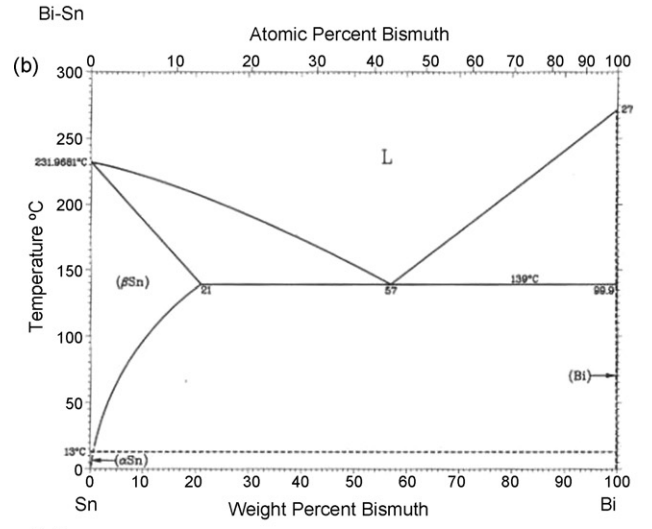
On the assumption that the particle size  $\eta$  and the macrostrain  $\varepsilon$  obey a Cauchy distribution [11], the following equation can be used [11]:

$$\frac{\beta \cos \theta}{\lambda} = \frac{1}{\eta} + \frac{2\varepsilon \sin \theta}{\lambda} \tag{2}$$

where  $\theta$  is the peak angle and  $\lambda$  is the wavelength of the used X-ray. From the analysis of the patterns of Fig. 2, the straight lines relating  $(\beta \cos \theta)/\lambda$  and  $(\sin \theta)/\lambda$  are given in Fig. 3(a–d) for all the tested samples. A half of the slope refers to the lattice strain  $\varepsilon$ , and the inverse number of the intercept at the ordinates, (y-axis), gives the average crystallite size  $\eta$  (nm), respectively. Applying Eq. (2), the obtained values of both the average crystallite size  $\eta$  (nm) and the lattice strain  $\varepsilon$  are given in Table 1.

The measured interplanar spacing d (nm) for the (200) plane of the R samples showed an increase of 0.009 nm for SnSb, a decrease of 0.005 nm for SnBi and 0.004 nm for SnZn with respect to Sn (N).





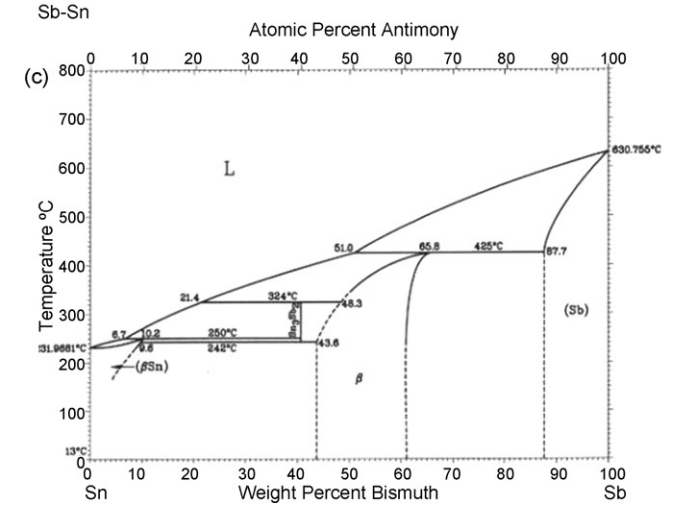


**Fig. 1.** The equilibrium phase diagram for: (a) tin–zinc, (b) tin–bismuth and (c) tin–antimony.

The cell volume for the binary cast alloys increases while it decreased for the R samples in the order from these containing Bi  $(r=0.156\,\mathrm{nm})$  to Sb  $(r=0.145\,\mathrm{nm})$  then Zn  $(r=0.131\,\mathrm{nm})$ , where r is the atomic radius. The same order exists for hardness as the bond length decreases for the larger atom and therefore binding increases.

## Download English Version:

# https://daneshyari.com/en/article/1580355

Download Persian Version:

https://daneshyari.com/article/1580355

<u>Daneshyari.com</u>